

Tuning the alignment of pentacene on copper substrate by annealing-assistant surface functionalization

Qiao-Jun Cao(曹巧君), Shuang Wen(温爽), Hai-Peng Xie(谢海鹏), Bi-Yun Shi(施碧云), Qun Wang(王群), Cong-Rong Lu(卢从蓉), Yongli Gao(高永利), Wei-Dong Dou(窦卫东)

Citation: Chin. Phys. B . 2020, 29(7): 076801 . **doi:** 10.1088/1674-1056/ab8da2
Journal homepage: http://cpb.iphy.ac.cn; http://iopscience.iop.org/cpb

What follows is a list of articles you may be interested in

Influence comparison of N_2 and NH_3 nitrogen sources on AlN films grown by halide vapor phase epitaxy

Jing-Jing Chen(陈晶晶), Jun Huang(黄俊), Xu-Jun Su(苏旭军), Mu-Tong Niu(牛牧童), Ke Xu(徐科)

Chin. Phys. B . 2020, 29(7): 076802 . **doi:** 10.1088/1674-1056/ab90ed

Epitaxial fabrication of two-dimensional $TiTe_2$ monolayer on Au(111) substrate with Te as buffer layer

Zhipeng Song(宋志朋), Bao Lei(雷宝), Yun Cao(曹云), Jing Qi(戚竞), Hao Peng(彭浩), Qin Wang(汪琴), Li Huang(黄立), Hongliang Lu(路红亮), Xiao Lin(林晓), Ye-Liang Wang(王业亮), Shixuan Du(杜世萱), Hong-Jun Gao(高鸿钧)

Chin. Phys. B . 2019, 28(5): 056801 . **doi:** 10.1088/1674-1056/28/5/056801

Controllable fabrication of self-organized nano-multilayers in copper-carbon films

Wei-Qi Wang(王伟奇), Li Ji(吉利), Hong-Xuan Li(李红轩), Xiao-Hong Liu(刘晓红), Hui-Di Zhou(周惠娣), Jian-Min Chen(陈建敏)

Chin. Phys. B . 2019, 28(3): 036802 . **doi:** 10.1088/1674-1056/28/3/036802

Effect of hydroxyl on dye-sensitized solar cells assembled with TiO_2 nanorods

Lijian Meng(孟立建), Tao Yang(杨涛), Sining Yun(云斯宁), Can Li(李灿)

Chin. Phys. B . 2018, 27(1): 016802 . **doi:** 10.1088/1674-1056/27/1/016802

Image potential states mediated STM imaging of cobalt phthalocyanine on NaCl/Cu(100)

Qinmin Guo(郭秦敏), Zhihui Qin(秦志辉), Min Huang(黄敏), Vladimir N. Mantsevich , Gengyu Cao(曹更玉)

Chin. Phys. B . 2016, 25(3): 036801 . **doi:** 10.1088/1674-1056/25/3/036801

Tuning the alignment of pentacene on copper substrate by annealing-assistant surface functionalization*

Qiao-Jun Cao(曹巧君)[1,†], Shuang Wen(温爽)[1,†], Hai-Peng Xie(谢海鹏)[2,†], Bi-Yun Shi(施碧云)[1], Qun Wang(王群)[1], Cong-Rong Lu(卢从蓉)[1], Yongli Gao(高永利)[3], and Wei-Dong Dou(窦卫东)[1,‡]

[1] *Laboratory of Low-dimensional Carbon Materials and Department of Physics, Shaoxing University, Shaoxing* 312000, *China*
[2] *Hunan Key Laboratory of Super Microstructure and Ultrafast Process, School of Physics and Electronics, Central South University, Changsha* 410083, *China*
[3] *Department of Physics and Astronomy, University of Rochester, Rochester, NY* 14627, *USA*

(Received 15 February 2020; revised manuscript received 5 April 2020; accepted manuscript online 28 April 2020)

Controlling the alignment and packing structure of organic molecules on solid substrate surfaces at molecule level is essential to develop high-performance organic thin film (OTF) devices. Pentacene, which is a typical p-type semiconductor material usually adopts lying-down geometry on metal substrates owning to π–d coupling between pentacene and metal substrates. However, in this study, we found that pentacene molecules can be adsorbed on an anneal-treated Cu (111) surface with their long axis perpendicular to substrate surface. Highly ordered single-layer pentacene film with stand-up molecular geometry was achieved on this substrate. It was found that the functionalization of Cu surface with C=O groups due to annealing treatment should be accounted for standing-up geometry of pentacene on Cu substrate. This observation shed light on the tuning of the alignment and packing structure of organic molecules.

Keywords: ultra-thin film, molecular alignment, metal substrate, interfacial tuning

PACS: 68.37.–d, 68.55.–a, 81.15.–z **DOI:** 10.1088/1674-1056/ab8da2

1. Introduction

Organic thin film (OTF) devices such as organic light-emit diodes (OLED), organic photovoltaic devices (OPV), and organic field-effect transistors (OFET), have been extensively noticed by science and industry field owning to their merits such as good flexibility, rich of colors, and low cost of fabrication.[1–11] Among these conventional OTF devices, OLED devices have begun to be industrialized, especially OLED displays have entered the market. In contrast, the industrial applications have not yet been realized for OPV and OFET devices. One of the factors that hinder the industrial applications of those devices is the low transport mobility of charge carriers or excitons within in OTF layers. It was well proved that the charge transport mobility can be remarkably increased by improving the crystallinity and modifying the molecular packing structures of OTF layers.[12,13] This has motivated numerous studies on OTF growth on various substrates such as metals, metal oxides, polymers, graphene, and graphene-like two-dimensional (2D) materials.[14–20]

Understanding and controlling the growth behavior of OTF on metal substrates are particularly important because OTF properties influence the charge transfer behavior between metal electrodes and OTF active layer. In general, π-conjugated organic molecules prefer to lie flatly on the metal substrate surface, especially on metal crystals such as Cu, Ag, Au, *etc*.[21–24] Pentacene, which has five fused benzene rings usually, takes lying-down geometry on atomically flat metal surfaces due to the π–d-like molecule–substrate interaction. In addition, the lying-down geometries were also observed for organic molecules on graphene and other 2D material substrates.[17,25–28] In those cases, the flatness of substrates and molecule–substrate electronic coupling jointly lead to lying-down geometry of organic molecules on these substrates. It is usually hard to make π-conjugated organic molecules to stand on the metal surfaces or graphene. Imperfections like steps, defects, and even contaminations on the substrate surface were reported to induce tilted geometries.[29–31] However, those treatments are either short of well-controlling or suffered from worse understanding.

In this study, we investigated the molecular alignment of pentacene on crystalline Cu substrates. We found that pentacene molecules take standing-up geometry on the anneal-treated copper substrate. In another words, the long-axis of pentacene is perpendicular to Cu substrate surface, leading to a thin film (TF) with molecular π–π stacking parallel to substrate surface. This observation is in discrepancy with the well reported lying-down geometry of organic molecules on metal surfaces. This study may provide a facile approach toward the tuning of the alignment and packing structure of organic

*Project supported by the Natural Science Foundation of Zhejiang Province, China (Grant No. LY19F040005) and the National Natural Science Foundation of China (Grant Nos. 61474077 and 51802355).

†These authors contributed equally to this work.

‡Corresponding author. E-mail: phyth@usx.edu.cn

© 2020 Chinese Physical Society and IOP Publishing Ltd

molecules on substrate even beyond metals.

2. Experimental and calculation details

2.1. Treatment of copper foil

Copper foils were bought from Alfa Asser. Two different purities of copper foils were used in the experiments, one with higher purity (HPC, 99.9999%,) and the other with lower purity (LPC, 99.8%). The annealing treatments of copper foils were performed on a home-made chemical vapor deposition (CVD) system.[32] This instrument is equipped with a furnace and a quartz tube. The background vacuum within the quartz tube is ~ 0.01 Pa. The copper foils were simply cleaned by cycles of rinsing in ethanol and DI water and then blow dried with nitrogen. The copper foils were folded into rectangular pocket and then loaded into the quartz tube for annealing treatments. Both foils were annealed according to the same procedure as shown in Appendix A: Supplementary materials (Fig. A1). Briefly, the temperature of the furnace was heated up to 1050 °C within 1 hour, and then keeping at this temperature for 6 hours. After that, the furnace was shut down and the temperature of the tube was cooled to room temperatures (RT) within 2 hours. It was found that Cu substates, especially the LPC substrates were passivated with –COOH groups upon the specific annealing treatment as being demonstrated by photoelectron spectroscopic measurements which will be shown in the latter section.

2.2. Deposition of pentacene

The annealed copper foils were cut into 1 cm×1 cm pieces before being loaded into ultra-high vacuum (UHV) chamber where pentacene in powder was deposited on to targeted substrate by using thermal evaporation method. The description of the UHV chamber can be found in literature.[33] Only the interior side of copper pocket was used for organic deposition. The copper substrates were pre-annealed at 150 °C in deposition chamber to remove possible air contaminations. Purified pentacene was thermally deposited onto copper substrates at a constant deposition rata of 0.5 nm/min. The substrates were kept at RT during organic deposition process.

2.3. Characterizations

Morphologies of metal substrates and the organic films were investigated using an atomic force microscopy (AFM) (Bruker multimode 8) with a taping-mode. And the crystalline structures of organic films were revealed by x-ray diffraction (XRD) measurements which were conducted with a Philips X'Pert XRD facility using Cu-$K\alpha$ emission. The alignments of pentacene were measured by Raman spectroscopy (Horiba HR evolution) equipped with a polarized 532-nm laser. A Zeiss Sigma 300 field-emission scanning electron microscopy (FE-SEM) was also used to characterize the surface properties of the annealed copper substrates. The chemical nature of copper substrates was characterized by using an Oxford energy dispersive spectrometer (EDS) and a Specslab2 x-ray photoelectron spectrometer.

3. Results and discussions

Figure 1(a) shows the AFM image of the anneal-treated LPC substrate. A height profile of the substrate surface along the line in the AFM image is shown in the bottom panel of Fig. 1(a). The height variation is lower than 0.5 nm across the measured region, indicating an atomically flat surface. Figures 1(b) and 1(c) show the AFM images of LPC samples after deposition of pentacene films with overall coverage of 0.4 monolayer (ML) and 1.0 ML, respectively. At sub-monolayer coverage, pentacene molecules prefer to nucleate into discrete islands with unique thickness (see Fig. 1(b)). The height profile shows that the height of pentacene island is ~ 1.5 nm. This value is well agreed with the van-der Waals dimension of pentacene,[34] *i.e.*, along the long axis of pentacene. This indicates that pentacene molecules adopt standing-up geometry on the anneal-treated LPC substrate. This observation seems to be unexpected since π conjugated organic molecules usually lie flatly on metal surface due to π–d-like molecule substrate interaction.[20–23] The pentacene islands grew larger as the coverage increased, and the neighbored islands gradually joined into each other, forming a flat film with one molecular thickness (see AFM image and height profiles shown in Fig. 1(c)). We noted that although the substrate surface was decorated by some defects, *e.g.*, trenches and protrusions, the imperfections seem to have negligible influence on the growth of pentacene. Figure 2(a) shows a defect point (see the arrow marked region) on LPC substrate surrounded by pentacene grain where the morphology is quite close to the grains at defect-free regions. Figure 2(b) shows the three-dimensional (3D) AFM image of pentacene islands on anneal-treated LPC substrate. These islands have similar height values, irrespective of the surface defects of Cu substrate.

For comparison, we show in Figs. 2(c) and 2(d) the 2D and its corresponding 3D AFM images of pentacene film on the anneal-treated HPC substrate. The nominal thickness of pentacene is the same as the one shown in Fig. 2(a). On HPC substrate, pentacene nucleated into individual islands which are much smaller in size than that of pentacene on LPC substrate grains, indicating dewetting nature of HPC substrate. This result implies that the growth mode and even the molecular orientation of pentacene on HPC substrate is different to that of pentacene on LPC substrate. The polarized Raman spectroscopy was used to identify the molecular orientation of pentacene on Cu substrates. Figures 2(e) and 2(f) show the Raman spectra for a 1.0-nm thick pentacene

film on the anneal-treated LPC and HPC substrates, respectively. According to the literature, the features at 1533 cm^{-1}, 1501 cm^{-1}, 1457 cm^{-1}, 1409 cm^{-1}, 1371 cm^{-1}, 1178 cm^{-1}, and 1158 cm^{-1} can be assigned to the A_g fundamental band, while the band at 1596 cm^{-1} can be assigned to a B_{3g} fundamental.[35] These Raman features originate from various vibrational modes of the C–H and C–C bonds of pentacene. It was previously demonstrated that the B_{3g} bands have zero Raman intensity when the long axis of pentacene is perpendicular to the electric vector of the laser beam used in the Raman measurements. On the contrary, A_g bands are undetectable when the long axis of pentacene is parallel to the electric vector of laser. For the case of pentacene on LPC substrate, Raman features of A_g bands dominated the Raman spectrum. This indicates that the long axis of pentacene is perpendicular to the electric vector of laser beam. Since the laser was incident in normal direction of substrate, these features indicate that the long axis of pentacene is perpendicular to Cu substrate surface. This conclusion is in good consistent with the above-mentioned AFM results. In contrast, E_{3g} bands at 1596 cm^{-1} was obviously observed for the case of pentacene on HPC substrate, indicating that the molecular plane of pentacene is parallel to HPC substrate. It was reported that ratio of intensity of 1596 cm^{-1} band to the intensity of 1533 cm^{-1} band ($R = I_{1593}/I_{1533}$) can be used to identify the lying geometry of pentacene on Cu substrates.[36] The R value is as small as 0.47 for the former case, while it is as large as 10.98 for the later. This implies that the alignment geometry of pentacene on LPC substrate is significantly different to that of the case of pentacene on HPC substrate even though the substrates were treated in the same way.

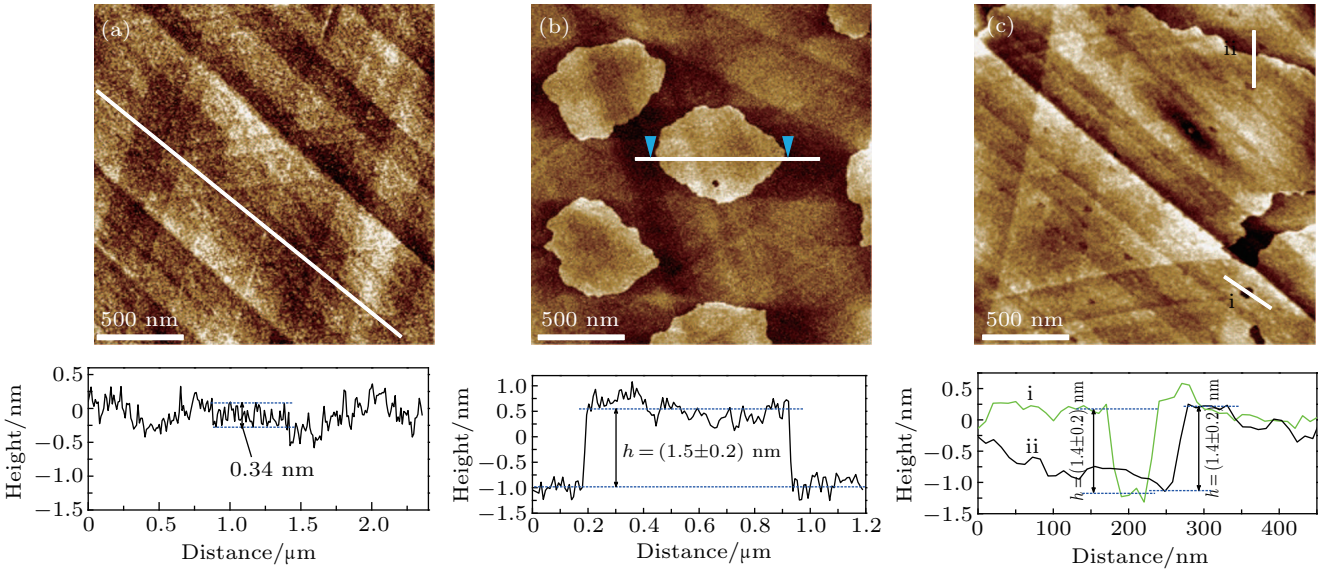


Fig. 1. AFM images of bare LPC and pentacene films on LPC substrates: (a) bare LPC, (b) pentacene of 0.4 ML on LPC, (c) pentacene of 1.0 ML on LPC substrate. The curves shown at the bottom of each panel are the height profiles taken from the regions marked with the solid lines shown in panels (a)–(c).

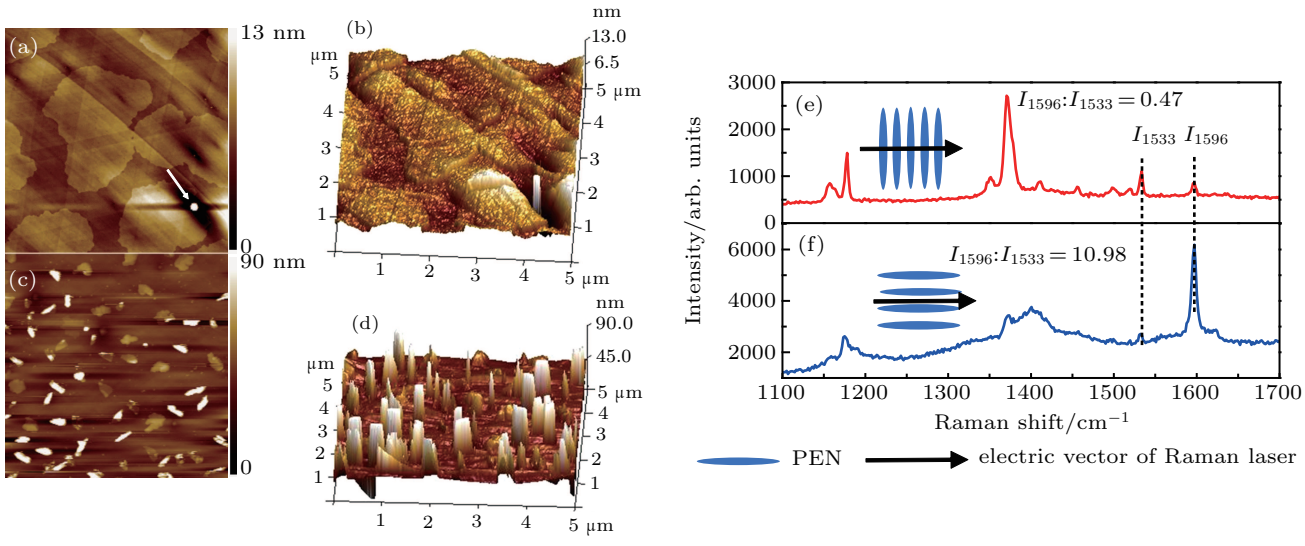


Fig. 2. Film morphology and molecular orientation of pentacene on anneal-treated LPC and HPC substrates: 2D (a) and 3D (b) AFM images of pentacene on LPC substrate; 2D (c) and 3D (d) AFM images of pentacene on HPC substrate; (e) Raman spectrum of pentacene film on LPC and (f) HPC substrates. The nominal thickness of pentacene film for all cases is 1.0 nm.

Figure 3(a) shows the AFM image of a pentacene film of 50 nm thickness on LPC substrate. Cone-shaped grains with typical size of 1 μm were observed. Layer-by-layer molecular stacking structure can be identified for each pentacene grain. The islands became narrower as the thickness of pentacene film increase, resulting in a large amount of edges and steps shaping the morphology of pentacene grain borders. Based on this morphology, Stranski–Krastanov growth mode can be established for the case of pentacene on LPC substrate. The corresponding x-ray diffraction (XRD) results are shown in Fig. 3(b). Five reflex peaks are revealed at 5.7°, 11.4°, 17.1°, 22.8°, and 28.5°.

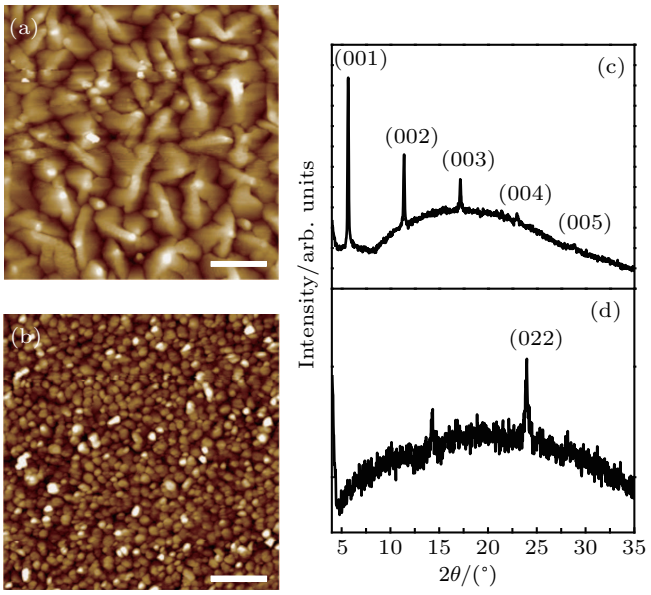


Fig. 3. Morphology and structure of pentacene film of thick layer on LPC and HPC substrates: AFM images of pentacene on LPC (a) and HPC (b) substrates show XRD results of pentacene films on LPC (c) and HPC (d) substrates. The scale bar in both of the AFM images is 1 μm for both panels (a) and (b). The nominal thickness of pentacene is 50 nm for both cases.

According to literature, all of these reflex peaks are originating from (001) lattice plane.[37–41] For the XRD measurements, we used Cu anode with wavelength of 1.5405 Å. Based on diffraction function, the interlayer distance of pentacene film on LPC substrate was evaluated to be 15.5 Å. This value is good consistent with the measured step height of single-molecule-thick pentacene island shown in Fig. 1. This indicates that the standing-up geometry of pentacene is succeeded in thick layer, leading to a π–π stacking of pentacene parallel to substrate surface. In contrast, the grain size of pentacene on HPC is much smaller than that of pentacene on LPC substrate. The XRD result show a weak peak at $2\theta = 24°$, which correspond to the interlayer distance of 3.79 Å, indicating a lying down geometry of pentacene with a molecular plane parallel to the substrate surface. Thereby, a perpendicular π–π stacking mode, *i.e.*, the molecular π–π direction normal to the substrate surface can be established for the case of pentacene film on HPC substrate. This geometry corresponds to the island-like domains, which begin to show up when pentacene is deposited onto the anneal-treated HPC substrate. This observation agrees well with the aforementioned AFM and Raman results. Base on the morphology of pentacene at initial deposition and thin film regime, a Volmer–Weber growth mode can be established for pentacene film on HPC substrate.

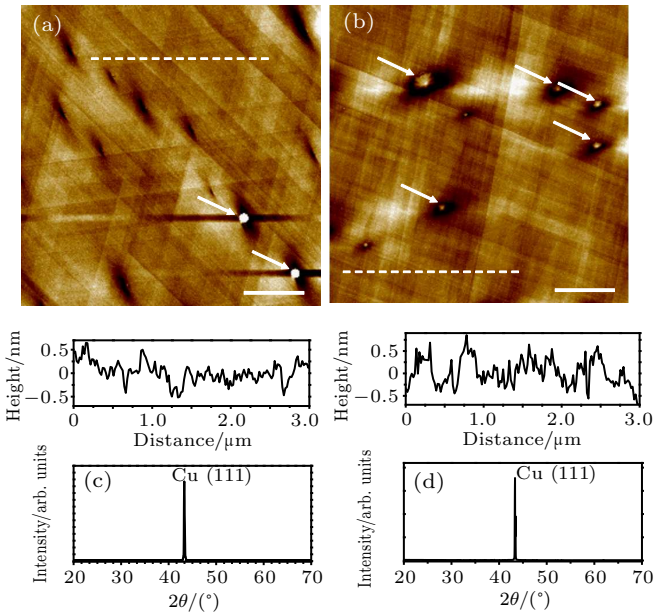


Fig. 4. Surface morphology and crystalline structure of the anneal-treated LPC and HPC substrates: AFM images of LPC (a) and HPC (b) substrates, respectively. The height profiles at the bottom panel show the height variation of the corresponding substrate surface. The height profiles were measured at the regions marked by the dotted lines in corresponding AFM images. XRD results show the crystallinity of the LPC (c) and HPC substrates (d). Only reflex peaks form (111) plane was obviously revealed for both cases.

To discovery the reasons account for the discrepancy in alignment geometry of pentacene on the anneal-treated LPC and HPC substrates, we investigate the physical and chemical natures of the substrates by using AFM and PES measurements. Figure 4 shows the surface morphology and crystalline property of the anneal-treated LPC and HPC substrates. AFM images shown in Figs. 4(a) and 4(b) reveals similar morphologies for both copper substrates. The height profiles along directions indicated by the dotted lines in the corresponding AFM images reveal height variation of ~ 0.3 nm. This value is close to the layer separation of Cu (111) substrate,[42] indicating an atomically smooth nature for both substrates. Although some defects such as trenches and protrusions are observed on both substrate surfaces, these defects barely affected the orientations of pentacene. In fact, pentacene islands can grow across these defects without changing the island thickness and nucleation behaviors (see the arrowed marked regions in Fig. 1(a)). In addition to the surface roughness, the crystalline structures of both copper substrate are almost the same either. Figures 4(c) and 4(d) show the XRD results of the anneal-treated LPC and HPC substrates, respectively. Both

substrates have single-crystalline nature of (111) phase as expected. This indicates that the physical properties of LPC substrate is almost identical to that of HPC substrate. These observations rule out the possibility to induce standing-up geometry of pentacene due to the imperfections of substrate surface such as roughness and defects.

Now, we turn our attention to the chemical properties of the anneal-treated copper substrates. The *ex-situ* x-ray photoemission spectroscopy (XPS) were collected to identify the elements and their chemical states on copper surface. Copper substrates were annealed at 120 °C for half an hour prior to XPS measurements to remove air contaminations. The XPS results of the anneal-treated Cu substrates were shown in Fig. 5. For both LPC and HPC samples, Cu_{2p}, C_{1s}, and O_{1s} core–level features were revealed. The Cu_{2p} spectrum reveals two typical features of pure coppers which are $2p_{3/2}$ at binding energy (BE) of 932.7 eV and $2p_{1/2}$ at BE of 952.6 eV, respectively. No obvious discrepancy in Cu_{2p} spectrum was observed for LPC and HPC samples. However, the C_{1s} and O_{1s} spectra of LPC substrates are completely different from that of HPC substrate (see Figs. 5(b)–5(c) and 5(e)–5(f). The signal to noise ratio of both C_{1s} and O_{1s} is very high for LPC sample, while it is very low for HPC sample. This discrepancy indicates that the concentration of carbon and oxygen on surface of LPC substrate is higher than that of HPC substrate. It is known that impurities such as carbon and oxygen are unavoidable in metals. However, it is reasonable to expect less concentration of the impurities for highly purified Cu than for the low purified ones. In this sense, the XPS observations agreed well with the common general knowledge. For LPC sample, the C_{1s} spectrum revealed two components at BE = 285.0 eV and 289.1 eV, respectively. According to literature, these peaks correspond to sp^2 carbon (C=C) and COOH components, respectively.[43] The observation of sp^2 component indicates that graphene-like units formed on surface of LPC substrate after annealing-treatment. The formation of graphene-like units is not surprising since the impurity carbon may segregate from bulk to the surface of Cu substrate during annealing process. In addition to graphene-like carbon units, amorphous carbon which has been widely reported to be unavoidable in CVD process was also been observed.[44–46] Similarly, both sp^2 C components were also observed in the case of HPC. Nevertheless, the intensity of both sp^2 C components is much lower than that of the LPC case. The obvious difference between C_{1s} spectrum of LPC and HPC substrates is that no COOH component was observed for the case of HPC substrate. The absence of COOH component in the case of HPC substrate is expectable because of the high-quality nature of HPC substrate. The observation of COOH component for the case of LPC sample indicates that the surface of LPC substrate was decorated by hydrocarbon materials having –COOH end groups. In contrast, no such component was observed for C_{1s} spectrum of HPC sample. The existence of –COOH component on LPC substrate was further demonstrated by the observation of C=O peak at BE = 531.4 eV in the O_{1s} spectrum of LPC substrate. No such component was observed in O_{1s} spectrum of HPC substrate. We noted that XPS feature originating from partially oxidation state of Cu was also revealed for both LPC and HPC samples. This feature may originate from defected positions on Cu surface, for instance the regions marked by arrow in Figs. 2 and 4. The energy dispersive x-ray (EDX) spectra shown in Fig. A2 in Appendix A verify the oxidation of Cu at these defected positions. Recalling the fact that the packing structure and nucleation behavior of pentacene on LPC substrate is completely different to that of pentacene on HPC substrate. Based on these observations, we conclude that the existence of COOH component should be account for the standing-up geometry of pentacene on LPC substrate.

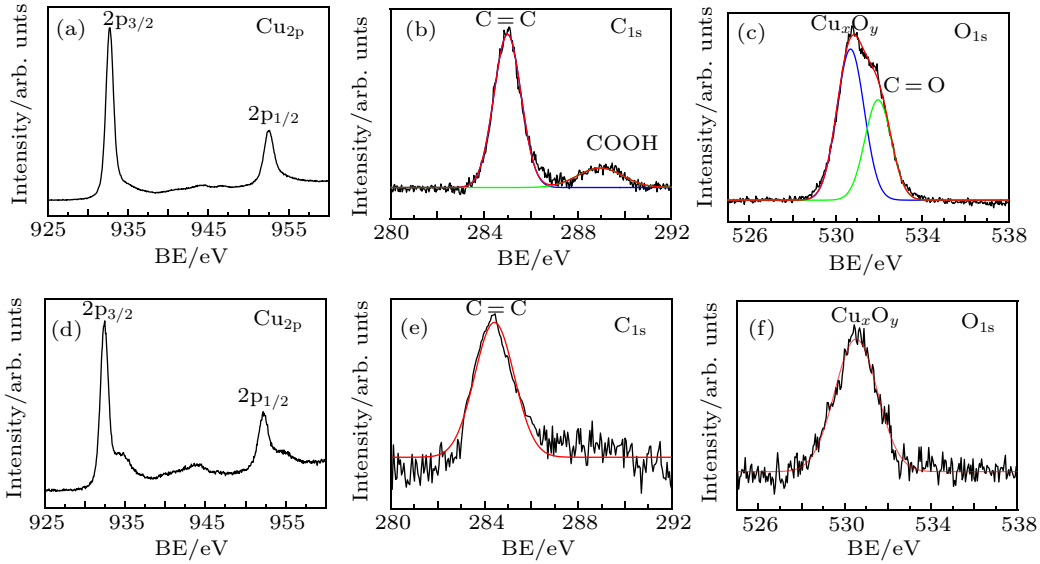


Fig. 5. XPS results of the anneal-treated Cu_LP [(a)–(c)] and Cu_HP [(d)–(e)] substrates.

The film growth scenario observed in this study parallels with the cases of pentacene on inert substrates such as SiO_2,[39] Al_2O_3,[47] highly oriented pyrolytic graphite,[34] and self-assembled monolayer-modified metal substrate.[48] In these cases, the intramolecular interaction between pentacene dominates monolayer-substrate interaction which favors the thermodynamically most stable (001) orientated film.[49] In our case, it is expected that the atomically smooth surface of copper substrate was covered by a monolayer of –COOH groups after the specific anneal-treatment. This suspicious was confirmed by the uniform film morphology of pentacene, *i.e.*, the 2D growth on LPC substrate. Otherwise, 3D grains may existence with the 2D ones since the surface nature would be nonuniform in a case of Cu substrate with partial –COOH coverage. The existence of –COOH functional groups act as decoupling layer which weakening the molecule-substrate interaction between pentacene and Cu (111) surface. So, the adsorption energy of pentacene on –COOH modified Cu substrate is expected to be much weaker than that of pentacene on fresh Cu substrate. This rather weak adsorption energy enables the standing-up/tilted geometry of pentacene at the interface thus allows the formation of orderly packed pentacene monolayer on the –COOH modified Cu substrate by suppress any grain due the lattice mis-match between pentacene and Cu substate. It is well known that the delicate balance between intramolecular interaction and molecule-substate interaction directs the formation of film with uniform morphology and crystalline structure. Thus, the growth mode will be varied provided the surface nature of substrate is nonuniform. For instance, Volmer–Weber (VW) growth rather than Frank–van der Merwe (FM) mode will appear if Cu surface was only partially covered by –COOH functional groups. Figure 6 shows the AFM image of pentacene film on a specific LPC substrate which was post annealed at 750 °C for deferent duration time in UHV chamber under H_2 partial pressure of 1.5×10^{-3} Pa. By conducting the post annealing procedure, the coverage of –COOH groups on LPC substrate was supposed to be decreased due to either thermal desorption or chemical reduction. This leads to the nonuniformity of chemical nature of LPC substrate. As was shown in Fig. 6, the growth behavior of pentacene film gradually changed from FM mode to a VW-dominated mode as the annealing duration time increases. This phenomenon further supports our conclusion that –COOH groups on substrate are responsible for the standing-up geometry. Nevertheless, further study is still needed to quantify the relation between growth scenario of pentacene film and the coverage of –COOH function groups.

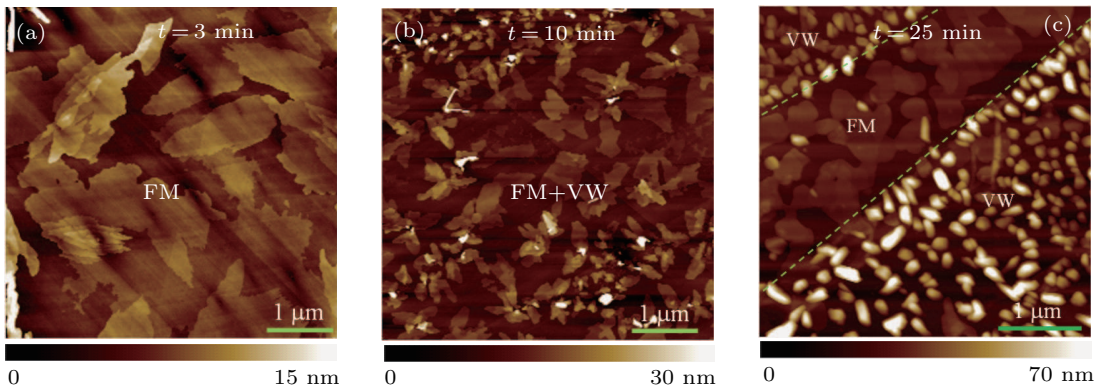


Fig. 6. AFM images of pentacene on post-anneal treated LPC substrates. The annealing duration time (t) is 3 min (a), 10 min (b), and 25 min (c). The nominated thickness of pentacene is 3 nm for all cases shown in this figure. The deposition condition of pentacene is the same as shown in other figures.

4. Conclusions

The molecular orientations of pentacene on Cu substrates were investigated by using AFM, Raman, SEM, and XPS measurements. It was found that pentacene adopts lying-down geometry on the anneal-treated highly purified Cu substrate. In contrast, pentacene molecules adopt standing-up geometry on the low purity Cu even though the annealing treatment is the same as that of the highly purified Cu substrate. A single molecular layer of pentacene film was achieved on the anneal-treated low purity Cu substrate. AFM and XPS investigations reveal that the surface of low purity Cu substrate was dressed with functional groups ended with –COOH functional group. Nevertheless, no such functional group was observed for the case of highly purified Cu substrate. This finding establishes the role of –COOH groups to induce the standing-up geometry of pentacene on metal substrate. In addition, this observation also sheds light on tuning of the molecular orientation of small conjugated organic molecules on other smooth and conductive substrate such as graphene.

Appendix A: Supporting information

The additional information for schematic procedure of annealing treatment, SEM, and EDX results of annealed Cu substrates are shown in Figs. A1 and A2.

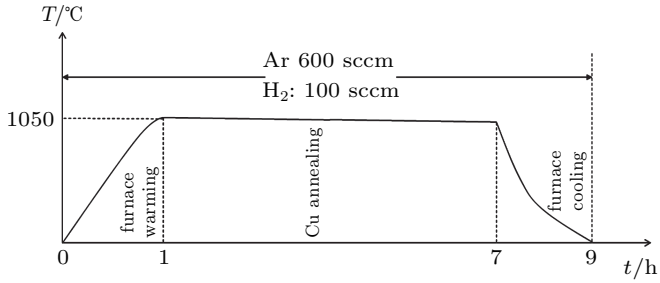


Fig. A1. Schematic program for the anneal-treatment of copper foil. Previous study had demonstrated that the anneal-treatment induced the recrystalline of copper foil 1.[50]

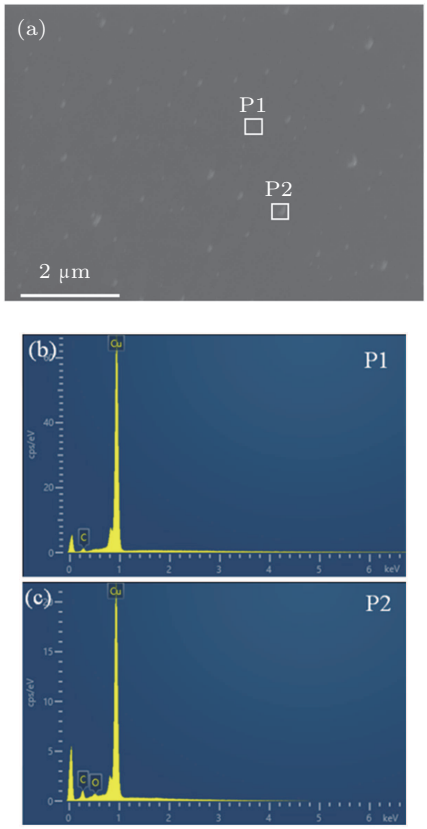


Fig. A2. SEM image and EDX results of the anneal-treated copper foil of low purity. The EDX spectra were collected from the positions marked by the white square. Oxygen on copper surface was clearly revealed at the defected regions which appears as white spots in SEM image.

References

[1] Lunt R R, Benziger J B and Forrest S R 2010 *Adv. Mater.* **22** 1233
[2] Park S K, Jackson T N, Anthony J E and Mourey D A 2007 *Appl. Phys. Lett.* **91** 063514
[3] Dimitrakopoulos C D and Malenfant P R L 2002 *Adv. Mater.* **14** 99
[4] Nakanotani H, Higuchi T, Furukawa T, Masui K, Morimoto K, Numata M, Tanaka H, Sagara Y, Yasuda T and Adachi C 2014 *Nat. Commun.* **5** 4016
[5] Han T H, Lee Y, Choi M R, Woo S H, Bae S H, Hong B H, Ahn J H and Lee T W 2012 *Nat. Photon.* **6** 105
[6] Kim K H, Liao J L, Lee S W, Sim B, Moon C K, Lee G H, Kim H J, Chi Y and Kim J J 2016 *Adv. Mater.* **28** 2526
[7] Uhrich C, Schueppel R, Petrich A, Pfeiffer M, Leo K, Brier E, Kilickiran P and Baeuerle P 2007 *Adv. Funct. Mater.* **17** 2991
[8] Wang K, Liu C, Meng T, Yi C and Gong X 2016 *Chem. Soc. Rev.* **45** 2937
[9] Hains A W, Liang Z, Woodhouse M A and Gregg B A 2010 *Chem. Rev.* **110** 6689
[10] Ju H, Knesting K M, Zhang W, Pan X, Wang C H, Yang Y W, Ginger D S and Zhu J 2016 *ACS Appl. Mater. Inter.* **8** 2125
[11] Han J and Wang J 2019 *Chin. Phys. B* **28** 017103
[12] Zhang Y, Qiao J, Gao S, *et al.* 2016 *Phys. Rev. Lett.* **116** 016602
[13] He X, Zhu G, Yang J, Chang H, Meng Q, Zhao H, Zhou X, Yue S, Wang Z, Shi J, Gu L, Yan D and Weng Y 2015 *Sci. Rep.* **5** 17076
[14] Zacher D, Shekhah O, Woll C and Fischer R A 2009 *Chem. Soc. Rev.* **38** 1418
[15] Kroger I, Stadtmuller B, Stadler C, Ziroff J, Kochler M, Stahl A, Pollinger F, Lee T L, Zegenhagen J, Reinert F and Kumpf C 2010 *New J. Phys.* **12** 083038
[16] Bischoff F, Seufert K, Auwarter W, *et al.* 2013 *ACS Nano* **7** 3139
[17] Xiao K, Deng W, Keum J K, *et al.* 2013 *J. Am. Chem. Soc.* **135** 3680
[18] Colson J W, Woll A R, Mukherjee A, Levendorf M P, Spitler E L, Shields V B, Spencer M G, Park J and Dichtel W R 2011 *Science* **332** 228
[19] Kowarik S, Gerlach A, Hinderhofer A, Milita S, Borgatti F, Zontone F, Suzuki T, Biscarini F and Schreiber F 2008 *Phys. Stat. Sol.* **2** 120
[20] Ruiz R, Choudhary D, Nickel B, Toccoli T, Chang K C, Mayer A C, Clancy P, Blakely J M, Headrick R L, Iannotta S and Malliaras G G 2004 *Chem. Mater.* **16** 4497
[21] Dou W, Huang S, Zhang R Q and Lee C S 2011 *J. Chem. Phys.* **134** 094705
[22] Dou W, Zhu J, Liao Q, Zhang H, He P and Bao S 2008 *J. Chem. Phys.* **128** 244706
[23] Cheng Z H, Gao L, Deng Z T, Liu Q, Jiang N, Lin X, He X B, Du S X and Gao H J 2007 *J. Phys. Chem. C* **111** 2656
[24] Jiang Y H, Xiao W D, Liu L W, Zhang L Z, Lian J C, Yang K, Du S X and Gao H J 2011 *J. Phys. Chem. C* **115** 21750
[25] Oyedele A D, Rouleau C M, Geohegan D B and Xiao K 2018 *Carbon* **131** 246
[26] Lee W H, Park J, Sim S H, Lim S, Kim K S, Hong B H and Cho K 2011 *J. Am. Chem. Soc.* **133** 4447
[27] Ling X, Fang W, Lee Y H, Araujo P T, Zhang X J, Rodriguez-Nieva F, Lin Y, Zhang J, Kong J and Dresselhaus M S 2014 *Nano Lett.* **14** 3033
[28] Ye W G, Liu D, Peng X F and Dou W D 2013 *Chin. Phys. B* **22** 117301
[29] Koini M, Haber T, Werzer O, Berkebile S, Koller G, Oehzelt M, Ramsey M G and Resel R 2008 *Thin Solid Films* **517** 483
[30] Eremtchenko M, Temirov R, Bauer D, Schaefer J A and Tautz F S 2005 *Phys. Rev. B* **72** 115430
[31] Dou W D and Lee C S 2014 *Appl. Phys. Lett.* **105** 223110
[32] Cao Q J, Shi B Y, Dou W D, Tang J X and Mao H Y 2018 *Carbon* **138** 458
[33] Shi B Y and Dou W D 2017 *Thin Solid Films* **636** 723
[34] Götzen J, Käfer D, Wöll C and Witte G 2010 *Phys. Rev. B* **81** 085440
[35] Seto K and Furukawa Y 2012 *J. Raman Spectrosc.* **43** 2015
[36] Zhang L S, Roy S S, Hamers R J, Arnold M S and Andrew T L 2015 *J. Phys. Chem. C* **119** 45
[37] Girlando A, Masino M, Brillante A, Toccoli T and Iannotta S 2016 *Crystals* **6** 41
[38] Siegrist T, Kloc C, Schon J H, Batlogg B, Haddon R C, Berg S and Thomas G A 2001 *Angew. Chem.-Int. Edit.* **40** 1732
[39] Dimitrakopoulos C D, Brown A R and Pomp A 1996 *J. Appl. Phys.* **80** 2501
[40] Bouchoms I P M, Schoonveld W A, Vrijmoeth J and Klapwijk T M 1999 *Synth. Met.* **104** 175
[41] Kafer D, Ruppel L and Witte G 2007 *Phys. Rev. B* **75** 085309
[42] Guo J, Mo Y, Kaxiras E, Zhang Z and Weitering H H 2006 *Phys. Rev. B* **73** 3405
[43] Lin L, Zhang J C, Su H S, *et al.* 2019 *Nat. Commun.* **10** 1912
[44] Robertson J 1986 *Adv. Phys.* **35** 317
[45] Khaliullin R Z, Eshet H, Kühne T D, Behler J and Parrinello M 2011 *Nat. Mater.* **10** 693
[46] Li X, Cai W, Colombo L and Ruoff R S 2009 *Nano Lett.* **9** 4268
[47] Deman A L, Eroul M, Lallemann D, Phaner-Goutorbe M, Lang P and Tardy J 2008 *J. Non-Cryst. Solids* **354** 1598
[48] Yang H, Huang L, Sun K, Niu K, Cui Z, Zhang H, Wang Z, Yan D and Chi L 2017 *J. Phys. Chem. C* **121** 25043
[49] Choudhary D, Clancy P, Shetty R and Escobedo F 2006 *Adv. Funct. Mater.* **16** 1768
[50] Cao Q J, Shi B Y, Dou W D, Tang J X and Mao H Y 2018 *Carbon* **138** 458